



CrossMark
 click for updates

Cite this: *RSC Adv.*, 2016, 6, 50673

Construction and drug delivery of a fluorescent TPE-bridged cyclodextrin/hyaluronic acid supramolecular assembly†

Qian Zhao,^a Yong Chen,^a Mo Sun,^a Xian-Jing Wu^a and Yu Liu^{*ab}

A supramolecular assembly was successfully constructed from tetraphenylethylene-bridged β -cyclodextrin tetramers (TPECD) and adamantyl-grafted hyaluronic acids (HAAD) and fully characterized by UV-vis spectroscopy, fluorescence emission spectroscopy, zeta potential, SEM, AFM and TEM. The obtained TPECD–HAAD assembly, which existed as spherical nanoparticles with an average diameter of 50 nm, emitted stronger fluorescence than free TPECD due to the restricted intramolecular rotation. Significantly, this supramolecular assembly can efficiently load the anticancer drug doxorubicin (DOX) into cancer cells, and the resultant DOX@TPECD–HAAD system had higher anticancer ability and fewer side effects than free DOX.

Received 23rd March 2016
 Accepted 7th May 2016

DOI: 10.1039/c6ra07572j

www.rsc.org/advances

Introduction

The application of nanotechnology in the anticancer field has infinite potential for healthcare.^{1–5} The construction of targeting drug-delivery systems to increase the specificity for killing cancer cells while leaving healthy cells intact is an urgent matter, because cancer treatment paradigms mainly rely on whole body treatment with chemotherapy agents, exposing the patient to medication that non-specifically kills rapidly dividing cells, leading to many side effects.^{6–10} Because hyaluronic acid (HA) has some gratifying qualities, such as low toxicity, biocompatibility, biodegradability, and importantly its targeting ability due to the over-expression of HA receptors on the cell surface, HA-mediated site-specific drug delivery by HA-based supramolecular assemblies is becoming more and more popular among chemists.^{11–15} For example, Elisseff, Singh, and co-workers presented a polymer–peptide surface coating platform to non-covalently bind HA as a natural lubricant in the body to enhance the lubrication on tissue and biomaterial surfaces.¹⁶ Park, Kim, and co-workers used poly(ethylene glycol)-conjugated HA nanoparticles as carriers for anticancer drugs including DOX and CPT.¹⁷ On the other hand, Tang and co-workers discovered a class of molecules with aggregation-induced emission (AIE) properties due to the restriction of intramolecular rotation (RIR), among which tetraphenylethylene (TPE) stands out due to the facile synthesis and easy modification.^{18–21}

In this work, we attached β -cyclodextrin (β -CD), a torus-shaped cyclic oligosaccharide that can bind various inorganic/organic/biological molecules in both aqueous solution and the solid state,^{22–27} to the TPE core. Then, the resultant TPE-bridged β -CD tetramers (TPECD) were non-covalently associated with the adamantyl-grafted HA (HAAD) through the strong host–guest interaction between β -CD and adamantyl group to construct a water-soluble and biocompatible supramolecular assembly TPECD–HAAD (Scheme 1) with several inherent advantages as (1) the HA skeleton enabled the targeting ability of TPECD–HAAD, (2) the four β -CD molecules linked together by TPE could form a compact structure with HAAD through the host–guest complexation, (3) TPE could provide a hydrophobic microenvironment favorable to the loading of drug, and the twining structure of HA could prevent the leakage of loaded drug to some extent. As a result, the TPECD–HAAD assembly loaded with the anticancer drug doxorubicin (DOX) presented the higher anticancer ability and the lower side effect than free DOX.

Results and discussion

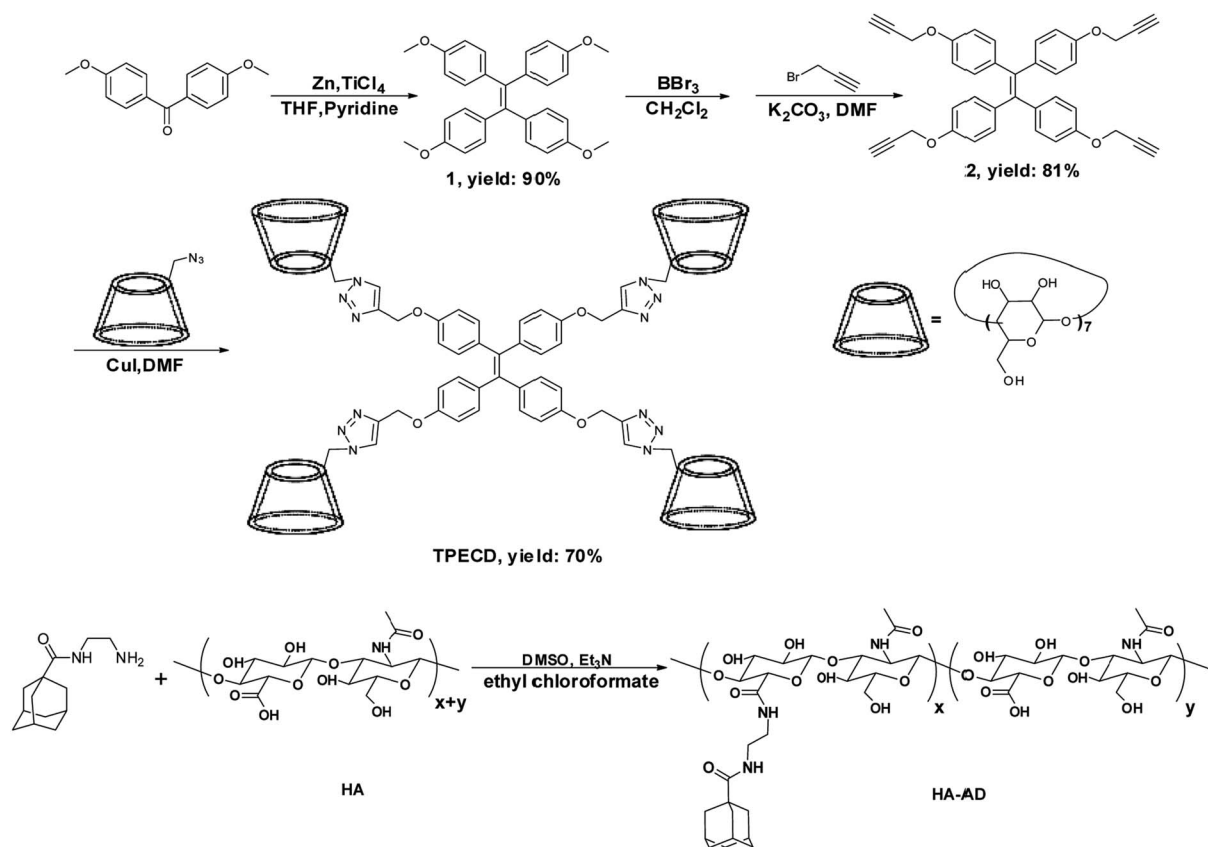
Synthesis of TPECD and HAAD

As shown in Scheme 1, TPE derivative **1** was prepared using the McMurry coupling of 4,4'-dimethoxybenzophenone, and then its demethylation with BBr_3 gave a kind of purple powder smoothly. A further treatment of the crude product with 3-bromo-1-propyne in the presence of K_2CO_3 afforded the propargyl-attached TPE derivative **2**.²⁸ The efficient transformation from **1** into **2** was confirmed by the appearance of resonance peaks of propargyl protons in the ^1H NMR spectrum after the reaction was completed. Subsequently, β -CDs were introduced onto TPE *via* a copper(I)-catalyzed click reaction

^aDepartment of Chemistry, State Key Laboratory of Elemento-Organic Chemistry, Nankai University, Tianjin, 300071, P. R. China. E-mail: yuliu@nankai.edu.cn

^bCollaborative Innovation Center of Chemical Science and Engineering (Tianjin), Nankai University, Tianjin, 300071, P. R. China

† Electronic supplementary information (ESI) available: Experimental details and characterization data. See DOI: 10.1039/c6ra07572j



Scheme 1 Synthetic route of TPECD and HAAD.

between **2** and azido-functionalized β -CD. The formation of triazole ring was confirmed by a clear ^1H NMR signal at 7.78 ppm (single peak, 4H). On the other hand, HAAD was

synthesized through an amidation reaction using a previously reported method.¹² By comparing the ^1H NMR spectrum of HAAD (Fig. S10[†]) with that of HA (Fig. S9[†]), the degree of

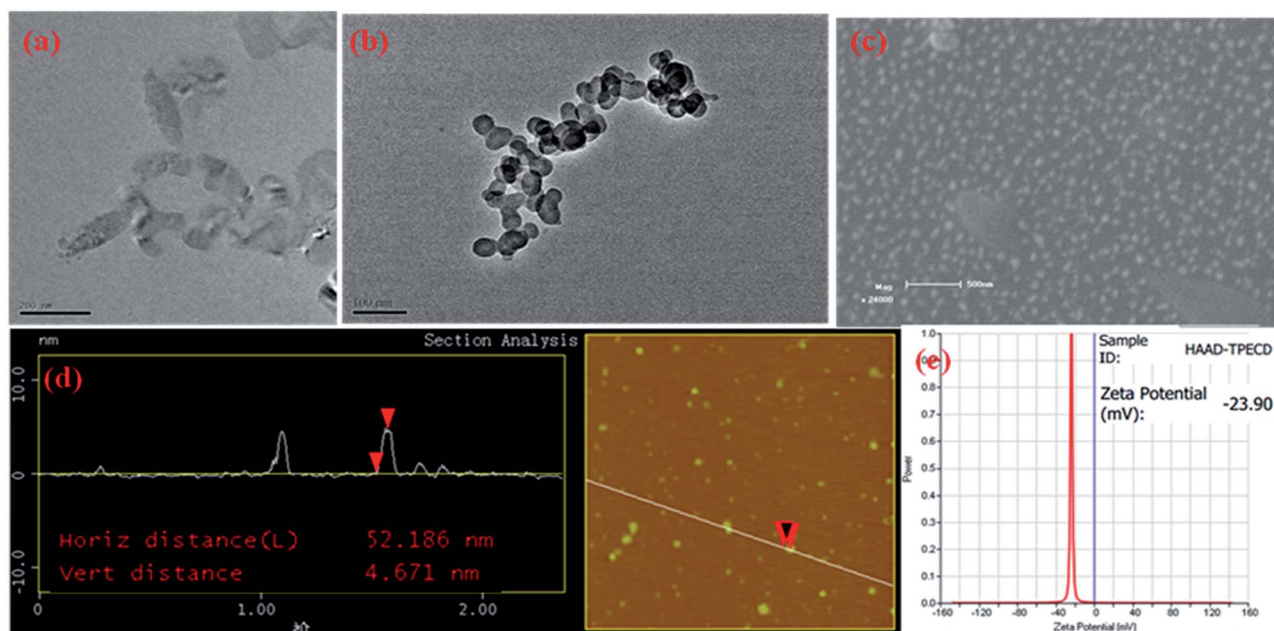


Fig. 1 (a) TEM images of HAAD. (b) TEM, (c) SEM and (d) AFM (e) ELS images of TPECD–HAAD assembly.

substitution (DS) was determined as 10% from the integrated peak area of adamantyl moiety and HA backbone using the single-point method. This value indicated that every 10 repeating sugar units in HA was grafted by an adamantyl group. Because at least six repeating units of HA are needed for achieving the multiple HA-CD44 interactions in the tumor-targeting bioconjugates bearing HA and cytotoxic agents, the resultant HAAD should have enough numbers of repeating units to interact with CD44.¹¹

Construction of TPECD-HAAD assembly

Owing to the strong binding of adamantyl groups with β -CD cavities,²⁹ the TPECD-HAAD assembly could be easily constructed by simply mixing TPECD and HAAD at a adamantyl group/ β -CD cavity ratio of 1 : 1 in aqueous solution, and its morphological and structural features was fully investigated by high-resolution transmission electron microscopy (HR-TEM), atomic force microscopy (AFM), scanning electron microscopy (SEM), and zeta potential experiments. In the HR-TEM images, the free HAAD mainly existed as the loose fusiform structures (Fig. 1a), while the TPECD-HAAD assembly existed as the spherical nanoparticles with an average diameter of 50 nm (Fig. 1b), and these particles tended to aggregate during the preparation process through hydrogen bonding interactions among the carboxylic and hydroxyl groups. SEM (Fig. 1c) and AFM (Fig. 1d) images gave the similar morphological information, showing many discrete spherical nanoparticles. Furthermore, the zeta potential was measured as -23.90 mV (Fig. 1e), indicating that the negatively charged surface of TPECD-HAAD assembly may have the capability of loading cationic drugs, and the serum environment would not seriously affect the stability of TPECD-HAAD.³⁰

Photophysical property

The UV-Vis spectra of TPECD at different concentrations (from 1 μ M to 10 μ M) were measured (Fig. S11[†]). The work plot at 316 nm showed a liner increase coinciding well with the Lambert-Beer's law. Similar phenomenon was also observed in the fluorescence spectra, where the fluorescence emission of TPECD linearly enhanced with increasing the concentration of TPECD from 1 μ M to 60 μ M (Fig. S12[†]). These results jointly confirmed that TPECD could not form self-aggregate under our experimental condition. On the other hand, the fluorescence emission intensity of TPECD-HAAD was nearly two times stronger than that of TPECD under the same condition. Moreover, under UV light (365 nm) irradiation, the TPECD-HAAD assembly gave a brighter blue fluorescence than TPECD (Fig. 2), and the quantum yield increased from 42.3% (TPECD) to 68.2% (TPECD-HAAD). In the control experiment, the fluorescence of TPECD nearly unchanged with the addition of free HA and 1-adamantanecarboxylic sodium. A possible reason for the enhanced fluorescence of TPECD-HAAD may be that the formation of nanoparticles restricted the intramolecular rotation of phenyl groups, which prevented the nonradiative decay of TPECD and thus enabled the enhanced luminescence.

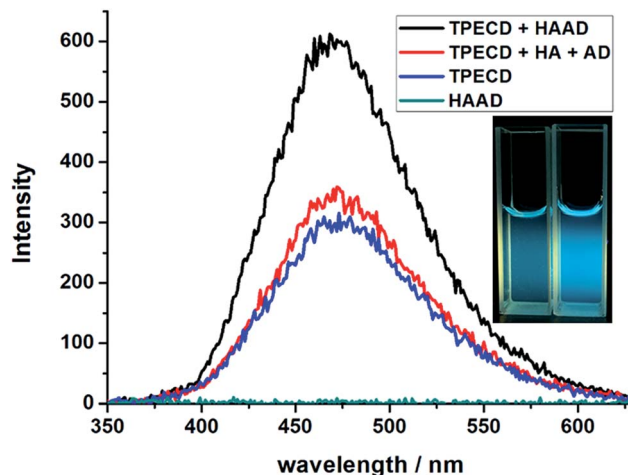


Fig. 2 Fluorescence emission spectra of TPECD-HAAD, TPECD, HAAD (ex = 330 nm) (inset: photo of TPECD (left) and TPECD-HAAD (right) under 365 nm irradiation).

Drug loading

The capability of TPECD-HAAD assembly on loading drugs was examined by using DOX, an efficient anticancer drug, as a model substrate, and its ϵ value in H_2O was measured as 13.71 $g^{-1} cm^{-1}$ at 481 nm. A new band at 481 nm, which was assigned to the characteristic absorption of DOX, appeared in the UV-vis spectrum of DOX@TPECD-HAAD (Fig. 3). The absorption of TPECD-HAAD as the reference was deducted from the UV-vis spectrum of DOX@TPECD-HAAD, and then the net concentration of DOX could be calculated according to the molar absorption coefficient at 481 nm. Therefore, the DOX loading efficiency and the encapsulation efficiency were calculated as 9.9% and 41.7%, respectively. Moreover, TEM images showed that the TPECD-HAAD assembly remained the original structural features after loading DOX.

Controlled drug release

The controlled release behaviors of DOX from DOX@TPECD-HAAD were examined using fluorescence spectroscopy within

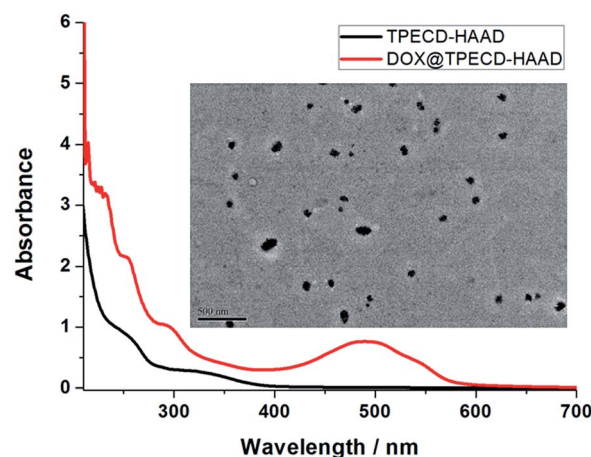


Fig. 3 UV-vis spectra of TPECD-HAAD assembly and DOX@TPECD-HAAD in H_2O (inset: TEM image of DOX@TPECD-HAAD).

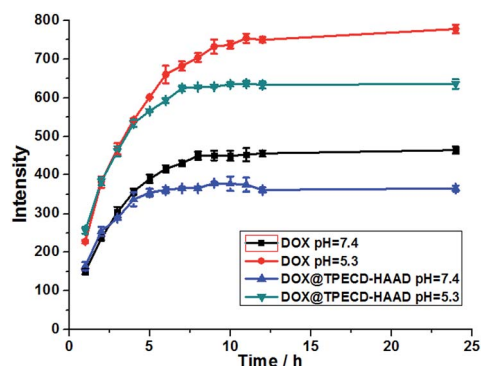


Fig. 4 *In vitro* DOX-release profiles from DOX and DOX@TPECD-HAAD assembly at different pH.

a period of 24 h at pH 7.4 and 5.3 because they are close to the physiological and endosomal pH values of a cancer cell, respectively. Fig. 4 showed that, at either pH 7.4 or 5.3, DOX@TPECD-HAAD presented a smooth and controlled release of DOX as compared with free DOX, and the drug release rate of DOX from DOX@TPECD-HAAD at pH 5.3 was measured to be faster than that at pH 7.4. This property would promote the bioactivity of DOX@TPECD-HAAD in a slightly acidic cancer cell environment.

Anticancer activity *in vitro*

Cytotoxicity experiments were also performed to evaluate the anticancer activity of DOX@TPECD-HAAD *in vitro* by using a 3-(4,5-dimethylthiazol-2-yl)-2,5-diphenyltetrazolium bromide (MTT) assay. After incubation with TPECD-HAAD at different concentrations (4, 8, 10, 40, or 60 μM) individually for 48 h, the normal fibroblast NIH3T3 cells and MCF-7 cancer cells remained a viability of >91% (Fig. 5 and S13[†]). These results revealed that the TPECD-HAAD assembly exhibited the low

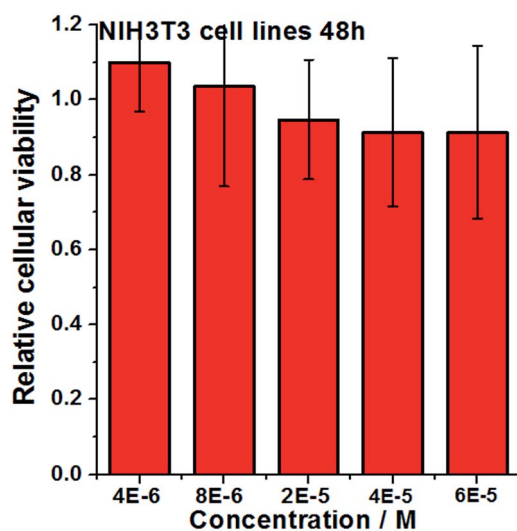


Fig. 5 *In vitro* cytotoxicity of TPECD-HAAD assembly (concentrations calculated according to TPECD).

cytotoxicity and good biocompatibility. Significantly, DOX@TPECD-HAAD displayed a higher anticancer activity toward MCF-7 cancer cells, a type of human breast cancer cells with abundant HA receptors being over-expressed on its surface (Fig. 6). After 48 h incubation, DOX@TPECD-HAAD gave a relative cellular viability towards MCF-7 cells as 25.4%, which was lower than the corresponding value of free DOX (38.3%). Furthermore, the half maximal inhibitory concentration (IC_{50}) was determined by an MTT assay, and the result showed that the DOX@TPECD-HAAD possessed a lower IC_{50} ($\text{IC}_{50} = 1.8 \text{ mg mL}^{-1}$) towards the MCF-7 cells than free DOX ($\text{IC}_{50} = 3.6 \text{ mg mL}^{-1}$) after incubation for 48 h. However, the anticancer activity of DOX@TPECD-HAAD obviously decreased (the relative cellular viability towards MCF-7 cells changed to 44.1%) when an excess amount of free HA was added because the saturation of HA-receptor on the surface of cancer cells with free HA

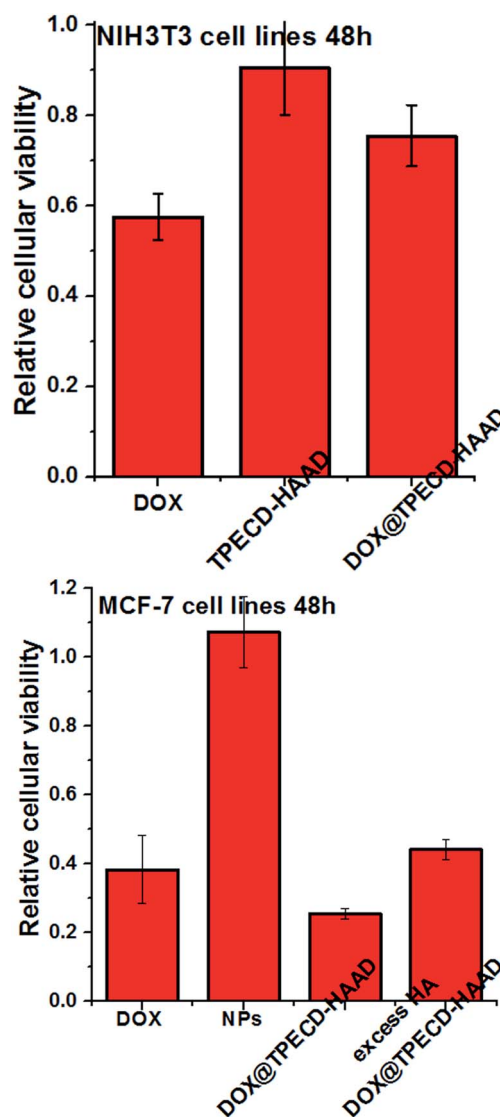


Fig. 6 Relative cellular viability of NIH3T3 and MCF-7 cell lines after 48 h of treatment with DOX, TPECD-HAAD, DOX@TPECD-HAAD or excess HA + DOX@TPECD-HAAD.

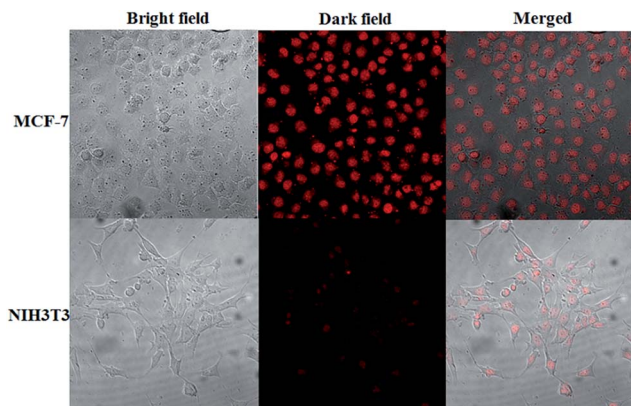


Fig. 7 Bright field (left), dark field (middle) and merged (right) images of MCF-7 (top) and NIH3T3 cells (bottom) incubated with DOX@TPECD-HAAD for 3 h.

molecules disfavored the interaction of HA-receptors with DOX@TPECD-HAAD. Moreover, the toxicity of DOX@TPECD-HAAD towards normal cells (the relative cellular viability 75.6% towards NIH3T3) was lower than that free DOX (the relative cellular viability 57.5% towards NIH3T3). These results jointly demonstrated the better anticancer activity and the lower side effect of DOX@TPECD-HAAD than those of free DOX. The efficient uptake of DOX into cancer cells was also confirmed by the fluorescent confocal microscopy. After incubation with DOX@TPECD-HAAD for 3 h, MCF-7 cancer cells showed the bright red fluorescence assigned to the luminescence of DOX. In sharp contrast, NIH3T3 cells exhibited only slight fluorescence under the same condition.

These phenomena demonstrated that DOX was efficiently loaded into cancer cells *via* the TPECD-HAAD assembly (Fig. 7).

Conclusions

By exploiting the strong host-guest complexation of β -CD cavity and adamantyl group, a nano-scaled supramolecular particle was successfully constructed from TPECD and HAAD, which could efficiently load anti-cancer drug into the cancer cells. Owing to the advantage of easy preparation, good water solubility, biocompatibility and biodegradability, this nanoparticle could act as a potential platform for drug-delivery, and its applications in therapy are still in process.

Experimental section

Instruments

NMR spectra were recorded on Bruker AV400 instruments. Mass spectra were performed on an MALDI-TOF mode MS. Transmission electron microscope (TEM) images were obtained on a Tecnai G2 F20 microscope (FEI) with an accelerating voltage of 200 kV. The samples were prepared by placing a drop of solution onto a carbon-coated copper grid and air-dried. For the AFM measurements, sample solution was dropped onto newly clipped mica and air-dried, and then the sample was examined using an atomic force microscope

(Veeco Company, Multimode, NanoIIIa) in tapping mode in the air under ambient conditions. Zeta potential was recorded on NanoBrook 173Plus (Brookhaven company) at 25 °C. The fluorescent confocal images were performed on a Leica TCS SP8 fluorescence microscope.

Synthesis of TPE derivative 2

Under nitrogen atmosphere, compound 1 (ref. 28) (3.00 g, 6.63 mmol) was dissolved and stirred in 40 mL of dry dichloromethane. BBr_3 (6.0 mL, 63.6 mmol) was added to the solution at 0 °C. After stirring for 30 min, the solution was allowed to warm to room temperature and stirred overnight. Cold water was added into the system under vigorous stirring until no more precipitate was formed. After filtration and drying, a purple solid was obtained. Then propargyl bromide (80 wt% in toluene, 6.0 mL, 54.0 mmol), K_2CO_3 (6 g, 43.5 mmol) and 100 mL of DMF were mixed with the crude product and refluxed overnight under nitrogen atmosphere. The mixture was then cooled to room temperature and filtered. After the removal of solvent under vacuum, the residue was purified by column chromatography on silica gel (ethyl dichloromethane/petroleum ether, $v/v = 1 : 1$) to give compound 2 as a white solid in 81% yield. ^1H NMR (400 MHz, DMSO): δ 6.88–6.84 (m, 8H), 6.77–6.73 (m, 8H), 4.71 (d, $J = 2.3$ Hz, 8H), 3.56 (t, $J = 2.3$ Hz, 4H).

Synthesis of TPECD

To the solution of 2 (60 mg, 0.11 mmol)²⁸ and β -CD azide²² (1 g, 0.86 mmol) in DMF, CuI (1 g, 5.25 mmol) was added as a catalyst. The mixture was stirred at 60 °C for 48 h, then concentrated and purified by column chromatography on silica gel (EtOH : $\text{NH}_3 \cdot \text{H}_2\text{O} : \text{H}_2\text{O} = 6 : 3 : 1$) to remove the excess amount of CuI. The resulting solution was dialyzed against an excess amount of water for 5 days. After being freeze-dried, TPECD was obtained as a slightly yellow solid in 70% yield. ^1H NMR (400 MHz, DMSO- d_6): δ 8.15 (s, 4H), 6.87 (dd, $J = 31.9, 8.0$ Hz, 16H), 5.95–5.57 (m, 64H), 5.23–4.27 (m, 84H), 4.06–3.48 (m, 111H). ^{13}C NMR (100 MHz, DMSO): δ 156.90, 142.92, 138.46, 136.92, 132.63, 126.26, 114.22, 102.40, 83.73, 82.00, 73.47, 72.72, 72.51, 61.24, 60.45, 59.50, 50.75. HRMS (MALDI-TOF): calculated for $\text{C}_{206}\text{H}_{304}\text{N}_{12}\text{O}_{140}\text{Na}$, 5210.70; found, 5210.70.

Synthesis of HAAD

Hyaluronic acid (1 g) was added into 100 mL of DMSO. After the polymer was completely dissolved, triethylamine (1.84 mL, 13.21 mmol) and ethyl chloroformate (0.76 mL, 8.0 mmol) were added, and the reaction solution was stirred at room temperature for 1 h. Then, adamantyl amine (293.2 mg, 1.32 mmol) was added, and the mixture was stirred at room temperature overnight. The solution was diluted with 100 mL of water and dialyzed (M_w cut off = 3500 Da) against water for 7 days. After dialysis, the sample was freeze-dried as a white powder. ^1H NMR (400 MHz, D_2O): δ 4.50 (s, 2H), 4.10–3.15 (m, 10H), 1.95 (s, 3H), 1.80–1.58 (m, 1H).

Loading of DOX

DOX@TPECD-HAAD were prepared according to the o/w method.^{31,32} Briefly, DOX·HCl (5 mg) was added to CHCl₃ (5 mL) and deprotonated by the addition of 3 equiv. TEA, followed by mixing for 2 h. TPECD (5.19 mg) and HAAD (15.99 mg) were dissolved in distilled water (50 mL). The CHCl₃ solution of DOX was added to the aqueous solution under vigorously stirring to form the o/w emulsion. The mixture was stirred under reduced pressure, allowing slow evaporation of CHCl₃. The solution was filtered through a syringe filter (pore size: 0.45 μm) to eliminate free DOX aggregates. The drug-loaded solution was lyophilized for future use. A series of DOX with different concentrations from 5 mg L⁻¹ to 70 mg L⁻¹ was measured, and the standard curve of DOX at 481 nm was did in order to get ε of DOX (Fig. S7†). Finally the drug loading efficiency was calculated through $m(\text{DOX in DOX@TPECD-HAAD})$ divided by $m(\text{DOX@TPECD-HAAD})$.

In vitro release of DOX

To further examine the drug release from DOX@TPECD-HAAD, 10 mg of DOX@TPECD-HAAD in 5 mL of buffer solution was placed in a dialysis bag (M_w cutoff = 3500 Da) and then dialyzed against 100 mL of PBS buffer (pH 7.2 and $I = 0.01$ M) or acetate buffer in an outer beaker at 37 °C. At each selected time interval, 3 mL of dialyzate was taken out from the beaker, and an equal volume of fresh PBS buffer was replaced to it. The released drug was evaluated by analysing the emission intensity of DOX at 481 nm.

Cell experiments

NIH3T3 cells and MCF-7 cancer cells were cultured in Dulbecco's modified Eagle's medium (DMEM) supplemented with 10% fetal bovine serum (FBS) at 37 °C under a humidified atmosphere with 5% CO₂. For the cytotoxicity experiments, NIH3T3 cells and MCF-7 cells were seeded in 96-well plates (1×10^5 cells per mL, 100 μL per well) for 48 h at 37 °C in 5% CO₂. The cells were incubated with DOX, TPECD-HAAD, DOX@TPECD-HAAD or DOX@TPECD-HAAD with excess HA ($2 \times [\text{HAAD}]$) for another 48 h. The concentration is 6×10^{-5} M, calculated according to TPECD, and DOX is added according to the loading efficiency. Then 50 μL of MTT solution (5 mg mL^{-1}) was added into each well. The cells were further cultured for 4 h, then the medium was removed, and 100 μL of DMSO was added into each well. After 15 min, the absorbance of the dissolved formazan was measured with a Bio-Rad micro plate reader at 485 nm. While for the confocal fluorescence image experiments, NIH3T3 cells and MCF-7 cells were seeded on 14 mm² cover slips that were placed in 6-well plates (2×10^5 cells per mL, 1 mL per well) for 24 h at 37 °C in 5% CO₂. The cells were incubated with DOX@TPECD-HAAD for 0.5 h or 3 h. Then the culture medium was removed, and the cells were washed with cold PBS solution for three times and fixed with 4% paraformaldehyde for 15 min. The cells were subjected to observation by a confocal laser scanning microscope.

Acknowledgements

We thank NNSFC (21432004, 21272125 and 91527301) for financial support.

References

- 1 W. T. Al-Jamal and K. Kostarelos, *Acc. Chem. Res.*, 2011, **44**, 1094.
- 2 M. E. Calderera-Moore, W. B. Liechty and N. Peppas, *Acc. Chem. Res.*, 2011, **44**, 1061.
- 3 Z. Ge and S. Liu, *Chem. Soc. Rev.*, 2013, **42**, 7289.
- 4 M. Vallet-Regi, M. Colilla and B. Gonzalez, *Chem. Soc. Rev.*, 2011, **40**, 596.
- 5 S. Mura, J. Nicolas and P. Couvreur, *Nat. Mater.*, 2013, **12**, 991.
- 6 K. Park, *ACS Nano*, 2013, **7**, 7442.
- 7 Z. J. Zhang, X. Zhang, X. H. Xu, Y. K. Li, Y. C. Li, D. Zhong, Y. Y. He and Z. W. Gu, *Adv. Funct. Mater.*, 2015, **25**, 5250.
- 8 S. Lee, H. Chen, T. V. O'Halloran and S. T. Nguyen, *J. Am. Chem. Soc.*, 2009, **131**, 9311.
- 9 X. Y. Zhong, K. Yang, Z. L. Dong, X. Yi, Y. Wang, C. C. Ge, Y. L. Zhao and Z. Liu, *Adv. Funct. Mater.*, 2015, **25**, 7327.
- 10 K. Shao, S. Singha, X. Clemente-Casares, S. Tsai, Y. Yang and P. Santamaria, *ACS Nano*, 2015, **9**, 16.
- 11 M.-Y. Lee, S.-J. Park, K. Park, K. S. Kim, H. Lee and S. K. Hahn, *ACS Nano*, 2011, **5**, 6138.
- 12 Y.-M. Zhang, Y. Cao, Y. Yang, J.-T. Chen and Y. Liu, *Chem. Commun.*, 2014, **50**, 13066.
- 13 D. Peer and R. Margalit, *Int. J. Cancer*, 2004, **108**, 780.
- 14 G. Bachar, K. Cohen, R. Hod, R. Feinmesser, A. Mizrahi, T. Shpitzer, O. Katz and D. Peer, *Biomaterials*, 2011, **32**, 4840.
- 15 N. Li, Y. Chen, Y.-M. Zhang, Y. Yang, Y. Su, J.-T. Chen and Y. Liu, *Sci. Rep.*, 2014, **4**, 4164.
- 16 A. Singh, M. Corvelli, S. A. Unterman, K. A. Wepasnick, P. McDonnell and J. H. Elisseeff, *Nat. Mater.*, 2014, **13**, 988.
- 17 K. Y. Choi, H. Y. Yoon, J.-H. Kim, S. M. Bae, R.-W. Park, Y. M. Kang, I.-S. Kim, I. C. Kwon, K. Choi, S. Y. Jeong, K. Kim and J. H. Park, *ACS Nano*, 2011, **5**, 8591.
- 18 J. d. Luo, Z. L. Xie, J. W. Y. Lam, L. Cheng, H. Y. Chen, C. F. Qiu, H. S. Kwok, X. W. Zhan, Y. Q. Liu, D. B. Zhu and B. Z. Tang, *Chem. Commun.*, 2001, 1740.
- 19 Y. Yang, Y.-M. Zhang, Y. Chen, J.-T. Chen and Y. Liu, *J. Med. Chem.*, 2013, **56**, 9725.
- 20 G. Liang, J. W. Y. Lam, W. Qin, J. Li, N. Xie and B.-Z. Tang, *Chem. Commun.*, 2014, **50**, 1725.
- 21 P. Wang, X. Yan and F.-H. Huang, *Chem. Commun.*, 2014, **50**, 5017.
- 22 M. Sun, H.-Y. Zhang, X.-Y. Hu, B.-W. Liu and Y. Liu, *Chin. J. Chem.*, 2014, **32**, 771.
- 23 H.-L. Sun, Y. Chen, J. Zhao and Y. Liu, *Angew. Chem., Int. Ed.*, 2015, **54**, 9376.
- 24 Z.-Q. Li, Y.-M. Zhang, Y. Chen and Y. Liu, *Chem.-Eur. J.*, 2014, **20**, 8566.

- 25 M. Sun, H.-Y. Zhang, B.-W. Liu and Y. Liu, *Macromolecules*, 2013, **46**, 4268.
- 26 Y. Lu, Q. Hu, Y. Lin, D. B. Pacardo, C. Wang, W. Sun, F. S. Ligler, D. D. Dickey and Z. Gu, *Nat. Commun.*, 2015, **6**, 10066.
- 27 Y. Yang, Y.-M. Zhang, Y. Chen, D. Zhao, J.-T. Chen and Y. Liu, *Chem.-Eur. J.*, 2012, **18**, 4208.
- 28 X.-M. Hu, Q. Chen, J.-X. Wang, Q.-Y. Cheng, C.-G. Yan, J. Cao, Y.-J. He and B.-H. Han, *Chem.-Asian J.*, 2011, **6**, 2376.
- 29 V. Rüdiger, A. Eliseev, S. Simova, H.-J. Schneider, M. J. Blandamer, P. M. Cullis and A. J. Meyer, *J. Chem. Soc., Perkin Trans. 2*, 1996, **10**, 2119.
- 30 Y. Yang, Y.-M. Zhang, Y. Chen, J.-T. Chen and Y. Liu, *J. Med. Chem.*, 2013, **56**, 9725.
- 31 L. Qiu, L. Zhang, C. Zheng and R.-J. Wang, *J. Pharm. Sci.*, 2011, **100**, 2430.
- 32 T. Wang, C. Zhang, X. J. Liang, W. Liang and Y. Wu, *J. Pharm. Sci.*, 2011, **100**, 1067.